ELSEVIER

Materials Science and Engineering A251 (1998) 135–141

MATERIALS SCIENCE & ENGINEERING A

Discontinuous coarsening of discontinuous precipitates in a Co–6 at.% Mo alloy

Shiu-Li Lee [a], Kuan-Ching Lee [a], Tung-Han Chuang [b,*]

[a] *Department of Physics, National Central University, Chung-Li, 32054, Taiwan, ROC*

[b] *Institute of Materials Science and Engineering, National Taiwan University, Sec. 4, 1 Roosevelt Road, Taipei, 10764, Taiwan, ROC*

Received 12 December 1997; received in revised form 13 March 1998

Abstract

The morphology and growth kinetics of the discontinuous coarsening of discontinuous precipitates in a Co–6 at.% Mo alloy have been investigated at temperatures ranging from 773 to 998 K by optical and scanning electron microscopy and X-ray diffraction. At all aging temperatures the alloy was observed to decompose completely by discontinuous precipitation into a fine lamellar structure of b.c.t. Co rich solid solution and an intermetallic compound phase of Co_3Mo. This lamellar structure was then decomposed at all aging temperatures by a discontinuous coarsening reaction. This reaction occurred at a much slower rate than the primary discontinuous precipitation reaction and resulted in a much coarser lamellar structure of the same phases. Through the measurements of the growth rates and lamellar spacings for both the discontinuous precipitation and discontinuous coarsening reactions, the grain boundary diffusion coefficients ($S\delta D_b$) were analyzed using the kinetic model of Petermann and Hornbogen. By comparison with the diffusion data in literature, it was concluded that the reactions were controlled by grain boundary diffusion in the reaction fronts of the discontinuous precipitates.

1. Introduction

Discontinuous precipitation (DP) [1] is a solid state reaction in which an initially homogeneous supersaturated solid solution (reactant) of (α_0) phase is decomposed into a two-phase ($\alpha+\beta$) lamellar structure, in the region behind the migrating reaction front and can be expressed by

$$\alpha_0 \rightarrow \alpha + \beta \quad (1)$$

where α represents the depleted solid solution phase, and β represents the precipitate. The conditions for the occurrence of DP are that the solvus composition is a function of temperature, and that large angle grain boundaries or a free surface of the solid be available. If no reactions other than DP are present to reduce part of the driving force, the reaction front will move with a constant speed in the isothermal transformation process.

After the primary DP reaction, the concentration of α-phase solid solution has not yet come to the equilibrium value. If the isothermal transformation process continues, a secondary reaction, i.e., the discontinuous coarsening (DC) [2] will take place, which will transform the fine-lamellar structure into a coarser lamellar structure of the same type:

$$(\alpha+\beta)_{\text{fine}} \rightarrow (\alpha'+\beta)_{\text{coarse}} \quad (2)$$

where α' is single phase, also with the crystal structure of α_0, but closer to the equilibrium concentration than α. The α'-phase solid solution lamellae are thicker than those of α, and the distance between α' lamellae (i.e., the thickness of β lamellae) is greater than that between α lamellae. The morphologies and growth kinetics of discontinuous coarsening have been investigated in many alloy systems, such as Fe–Ni–Ti [2], Zn–Al [13], Zn–Ag [14], Fe–Zn [15], Ni–In [16,17] and Ti–Al [18,19] et al. Recently, even its applications in developing TiAl intermetallic have also been reported [20,21]. However, the studies were scarce in Co-base alloys.

Supersaturated Co-rich cobalt–molybdenum alloys have been observed by Gust et al. [3] to decompose by DP during aging into a lamellar mixture of b.c.t. Co rich α' solid solution and an intermetallic compound phase β'' of Co_3Mo which has the same crystal structure as Ni_3Sn, and can be expressed as:

* Corresponding author. Tel.: +886 2 23929635; fax: +886 2 23634562.

0921-5093/98/$19.00
PII S0921-5093(98)00624-8

$$\alpha_0(\text{b.c.t.}) \rightarrow \alpha'(\text{b.c.t.}) + \beta''(Co_3Mo) \quad (3)$$

In the present work, the DC reaction to transform the discontinuous precipitates into coarser lamellae in a Co–6 at.% Mo alloy has been further studied. The growth rates and lamellar spacings of both of the DP and DC reactions have been measured. The grain boundary diffusion coefficients were then calculated using the kinetic model of Petermann and Hornbogen [6].

2. Experimental

The Co–6 at.% Mo alloy was prepared by being melted in a vacuum furnace and casted to produce ingots 10 mm in diameter and 100 mm in length. The alloy was first homogenized in the quartz tube at 1368 K for 533 h, then water-quenched to yield a final grain size 80 μm in diameter. The exact Mo-content is 9.41 ± 0.05 wt.%, which is near 6 at.%, as analyzed by X-ray fluorescence spectrometer.

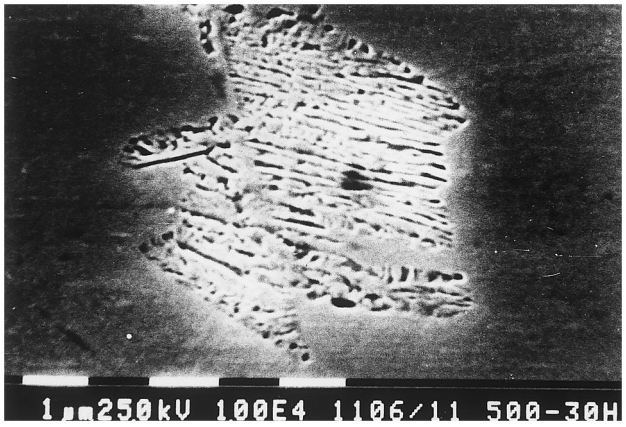

Fig. 1. Scanning electron micrography of Co–6 at.% Mo aged for 30 h at 773 K. Cells of lamellar discontinuous precipitation grew into the supersaturated phase.

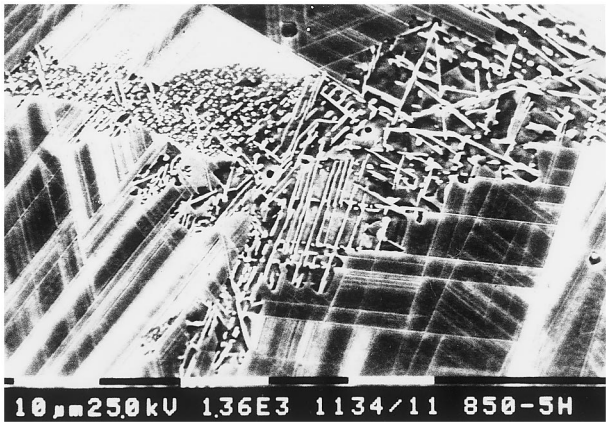

Fig. 2. Scanning electron micrography of Co–6 at.% Mo aged for 5 h at 1123 K. The granular and platlet structures occured at the region where the density of martensite boundaries is high.

Fig. 3. Scanning electron micrography of Co–6 at.% Mo aged for 74 h at 973 K. Coarse lamellar DC structure grew into fine lamellar DP structure.

Specimens of 3 mm in thickness were cut from the homogenized ingots, recapsulated and aged in the range of 733–1098K, then quenched in salt water at −5°C.

The aged specimens were then polished to 1200 grit, and etched in 60 ml of HCl, 15 ml of CH_3COOH, 15 ml of HNO_3, and 25 ml of H_2O for different time intervals depending on the types of observations to be made, e.g., 20–40 min for discontinuous precipitation, and 1–3 min for discontinuous coarsening. The growth rate measurements were made with optical microscopy, while the morphology and inter-lamellar spacing were determined with scanning electron microscopy (SEM).

The width of the cellular structure developing from grain boundaries was obtained by measuring the distance from the starting position of a cell to its leading edge. A total of 50 values of the seam width were taken and averaged for each aged specimen. The result was multiplied by $\pi/4$ to yield the true width for both DP and DC cell [4]. Then the growth rates for cells of DP and DC were obtained from the plots of the true width versus aging time, instructed as a function of the aging temperature. The inter-lamellar spacings of the precipitates in the cells of both DP and DC were taken as $\pi/4$ times the average of 40 spacings measured at each aging temperature for both DP and DC.

3. Results and discussion

3.1. Morphology

The typical morphology of discontinuous precipitates was shown in Fig. 1. The formation of lamellar structure of $\alpha' + \beta''$ (Co_3Mo) began at the grain boundaries and grew into the grain interiors. At higher aging temperatures, the untransformed region in the grain interiors revealed a highly stacking-faulted structure as shown in Fig. 2. In this case, the β'' (Co_3Mo) precipi-

tates grew with the same orientations as the stacking faults. This phenomenon is consistent with the observations in a commercial MM-302 cobalt base superalloy, that carbides can interact with stacking faults to create extensive precipitation in and around the faulted material [7].

After the primary DP reaction, when aging treatment continued, discontinuous coarsening precipitation began to take place from the grain boundaries (Fig. 3). During this reaction, the fine, closely spaced lamellar structure of the primary precipitates ($\alpha' + \beta''$) changed into a coarser and more widely separated lamellar structure ($\alpha'' + \beta''$), where α'' is closer to the equilibrium concentration of the solid solution at the aging temperature than the α' phase.

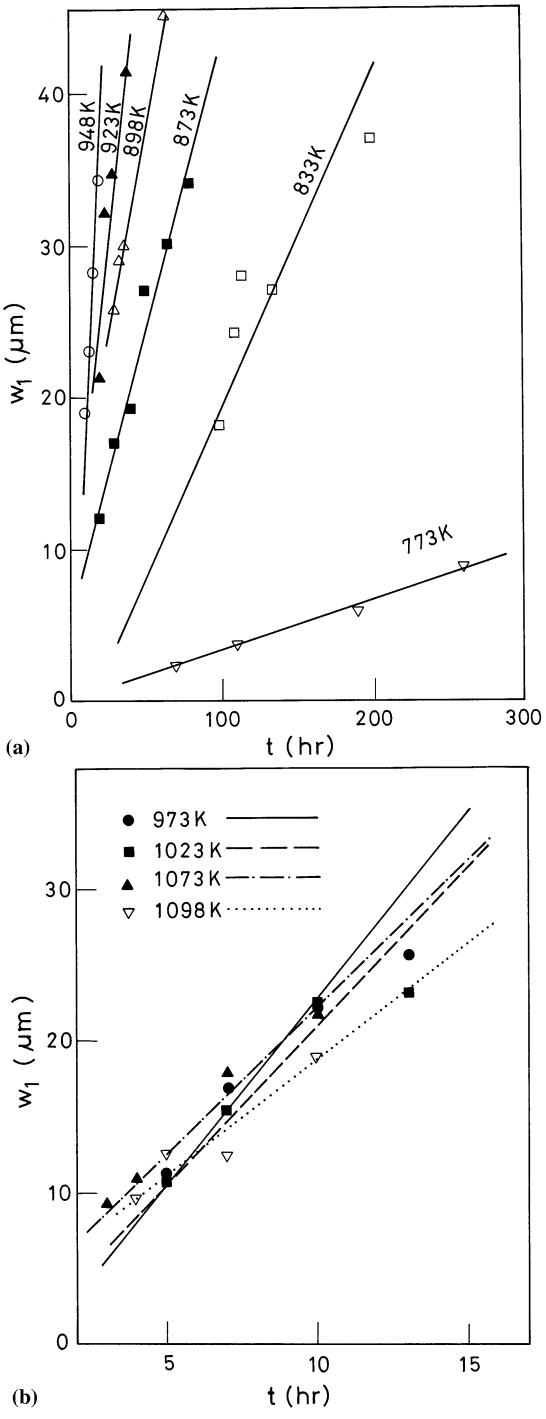

Fig. 4. The cell widths of discontinuous precipitation as a function of time at various temperatures.

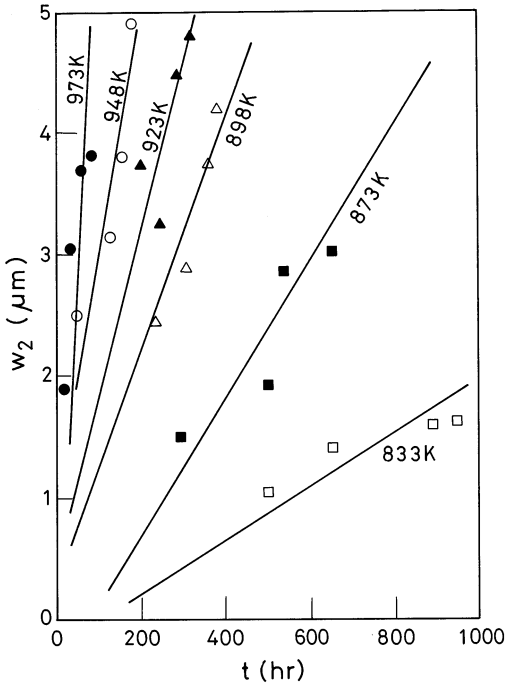

Fig. 5. The cell widths of discontinuous coarsening as a function of time at various temperatures.

In the early stage of DC the lamellar structure was not clear; with increasing aging time, the lamellar structure of $\alpha'' + \beta''$ gradually became regular (lamellae parallel to one another), but the orientations of the lamellae of the cells of DC were parallel, or inclined at an angle, or even perpendicular to those of the original cells formed during DP, i.e., the orientations of the lamellae of the cells of DC seemed to be irrelevant with respect to those of the original cells of DP. After a long period of aging treatment, bulk diffusion caused the continuous coarsening to appear at various temperatures. Also when the temperature was higher than 973 K, the continuous coarsening became compatible with the DC reaction.

3.2. Growth kinetics for DP and DC

The cell widths of DP and DC as a function of time at various temperatures were determined as shown in Figs. 4 and 5, and the cell growth rates, i.e., the velocities v_1 and v_2 of the reaction fronts of DP and DC were determined by the slope of the curves, which were summarized in Table 1. For Co–6 at.% Mo alloy, the cell width of DP was a linear function of time for a

Table 1
Cell growth rates v_1 and v_2, and lamellar spacings λ_1 and λ_2 for DP and DC reactions in Co–6 at.% Mo alloy

T (K)	v_1 (nm s^{-1})	λ_1 (μm)	v_2 (nm s^{-1})	λ_2 (μm)	$r=\lambda_2/\lambda_1$
833	6.944×10^{-11}	0.097	0.555×10^{-12}	0.580	5.98
873	1.389×10^{-10}	0.104	1.666×10^{-12}	0.635	6.11
898	2.222×10^{-10}	0.110	3.238×10^{-12}	0.684	6.22
923	3.333×10^{-10}	0.121	4.555×10^{-12}	0.748	6.18
948	5.555×10^{-10}	0.136	7.388×10^{-12}	0.820	6.03
973	7.222×10^{-10}	0.156	1.388×10^{-11}	0.900	5.77
1023	6.389×10^{-10}	0.236			
1073	5.556×10^{-10}				
1098	4.861×10^{-10}				

long aging period at lower temperature (over 300 h at 773 K), then the continuous precipitation began to take place to consume part of the driving force, and the growth rate then slowed down. The linear region became narrower as the temperature was raised higher (about 5 h at 1098 K), which might be due to the presence of the several types of reactions which would consume more driving force.

The reaction velocities of DP and DC, were represented as Arrhenius plots, which were shown in Fig. 6. It revealed that the cell growth rate of the reaction front of the DP cell increased with increasing aging temperature, reached the maximum at aobut 1017 K, then decreased monotonically as the temperature kept increasing, and exhibited a typical 'c' curve behavior. The highest reaction rate of DP occured at $T_{max}=1017$ K which was related to the solvus temperature, $T_{av}=1214$ K, by

$$T_{max}=0.84T_{av} \quad (4)$$

The constant 0.84 was in good agreement with the result of $T_{max}=(0.89\pm0.04)T_{av}$ [5], and was also quite close to the value $T_{max}=1016$ K obtained by Gust et al. [3] in measuring the same system. The cell growth rate of the reaction front of the DC cell, also increased monotonically with an increasing aging temperature from 833–973 K. At higher temperatures, the continuous coarsening obstructed the measurements of DC growth rate. Fig. 6 also showed that the cell growth rate of DC was about one order of magnitude smaller than that of DP at about 1000 K, and two orders of magnitude smaller than that of DP at about 830 K.

Data presented in Table 1 and Fig. 7 showed that the lamellar spacings λ_1 and λ_2 for both DP and DC increased monotonically with increasing aging tempera-

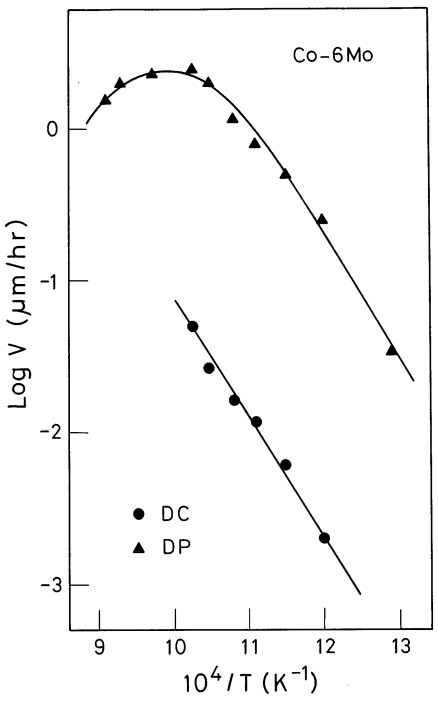

Fig. 6. Cell growth rates, v_1 and v_2, for discontinuous precipitation and discontinuous coarsening, respectively.

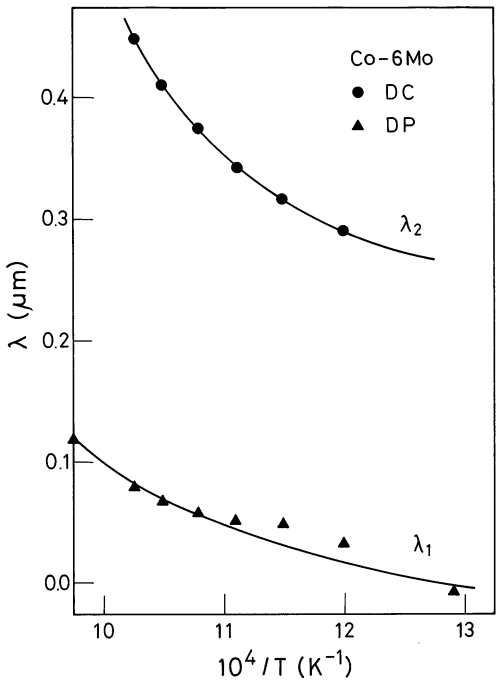

Fig. 7. Larmellar spacings, λ_1 and λ_2, for discontinuous precipitation and discontinuous coarsening, respectively.

Table 2
Free energy changes for the kinetic analyses of DP and DC reactions in Co–6 at.% Mo alloy

T (K)	ΔG_c^{DP} (Joule g-atom^{-1})	ΔG_σ^{DP} (Joule g-atom^{-1})	ΔG^{DP} (Joule g-atom^{-1})	ΔG^{DC} (Joule g-atom^{-1})
833	−427.31	55.51	−371.80	−46.22
873	−379.60	51.77	−327.83	−43.29
898	−380.83	48.95	−331.88	−41.07
923	−366.64	44.49	−322.15	−37.30
948	−337.14	39.59	−297.55	−33.02
973	−310.48	34.51	−275.97	−28.53
1023	−195.62	22.81	−172.81	
1073	−162.00			
1098	−86.02			

Table 3
Grain boundary diffusion coefficients for the DP and DC reactions in Co–6 at.% Mo alloy calculated from the theory of Petermann and Honbogen [6] in comparison with the volume diffusivities of Co in Co quoted from the data of Hirano et al. [11]

T (K)	$10^4/T$ (K^{-1})	$S\delta D_b$ (DP) (μm^3 h^{-1})	$S\delta D_b$ (DC) (μm^3 h^{-1})	D_v (Co–Co) (μm^2 h^{-1})
833	12.00	5.48×10^{-3}	1.26×10^{-2}	1.22×10^{-7}
873	11.45	1.50×10^{-2}	5.07×10^{-2}	7.55×10^{-7}
898	11.14	2.72×10^{-2}	1.24×10^{-1}	2.11×10^{-6}
923	10.83	5.23×10^{-2}	2.36×10^{-1}	6.00×10^{-6}
948	10.55	1.23×10^{-1}	5.34×10^{-1}	1.55×10^{-5}
973	10.28	2.32×10^{-1}	$1.43\times10^{+0}$	3.78×10^{-5}
1023	9.78	7.88×10^{-1}		2.12×10^{-4}

ture, and the coarsening ratios $r=\lambda_2/\lambda_1$ ranged from 5.8 to 6.2 for 560 K $\leq T \leq$ 700 K. Such a range of ratios was typical for the coarsening reaction. In addition, a slight temperature dependence of the coarsening ratios, i.e., they increased monotonically to a maximum then decreased again with increasing temperature, was observed, in the present study.

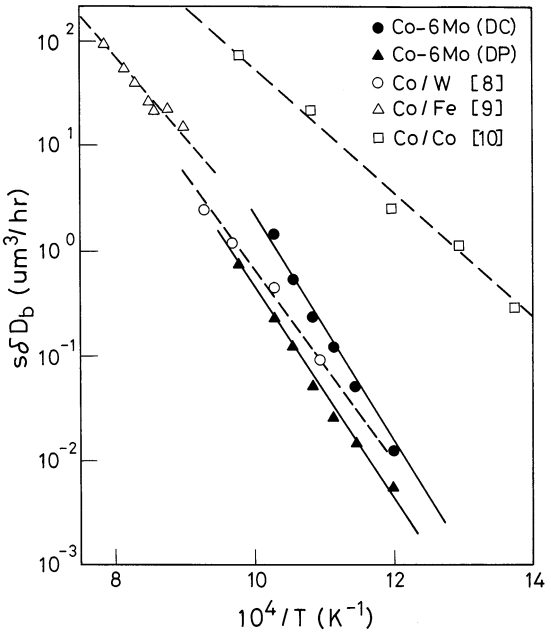

Fig. 8. Arrhenius plot of grain boundary diffusivities calculated from the kinetic analyses of discontinuous precipitation (DP) and discontinuous coarsening (DC) reactions in Co–6 at.% Mo alloy. For comparisons, the grain boundary diffusivities of W [8], Fe [9] and Co [10] in Co were also ploted.

According to the theory of Petermann and Hornbogen [6], the grain boundary diffusion coefficients can be obtained by:

$$S\delta D_b = -\frac{RT}{8\Delta G}\cdot v\lambda^2 \quad (5)$$

and

$$\Delta G^{DP} = \Delta G_C^{DP} + \Delta G_\sigma^{DP} = \Delta G_C^{DP} + 2\sigma V_m(1/\lambda_1)$$
$$\Delta G^{DC} = \Delta G_{min}^{DC} = 2\sigma V_m(1/\lambda_2 - 1/\lambda_1) \quad (6)$$

where ΔG is the free energy change, namely the driving force for the reaction, R is the gas constant, and T is the absolute temperature, and ΔG_c is the chemical free energy change, ΔG_σ is the interfacial free energy change, $\sigma = 4\times10^{-13}$ Joule μm^{-2} is the interfacial free energy per unit area as presented by Gust et al. [3,22], and $V_m = 6.73\times10^{12}$ μm^3 g^{-1} atom is the molar volume as calculated from the lattice constants of this alloy [23]. The calculated free energy changes were given in Table 2. The driving force for DC reaction was about one order of magnitude lower than that for the DP reaction. The lower driving force and larger diffusion path (lamellar spacing) for DC reaction resulted in a much slower growth rate of DC cells in comparison with the primary DP reaction.

The calculated grain boundary diffusion coefficients for both DP and DC reactions were given in Table 3.

Table 4
Arrhenius parameters experimentally determined from the kinetic analyses of DP and DC reactions in Co–6 at.% Mo alloy in comparison with those obtained from the grain bounday diffusion data of Co–W, Co–Fe and Co–Co in literature [8–10]

Systems	Temperature range (K)	$(S\delta D_b)_0$ ($\mu m^3\ h^{-1}$)	Q_b^{ef} (KJ $mole^{-1}$)	Reference
Co–6Mo(DC)	833–973	2.50×10^{11}	210.9	Present work
Co–6Mo(DP)	833–1023	6.54×10^{9}	194.2	Present work
Co–W	913–1073	2.79×10^{8}	165.3	[8]
Co–Fe	1100–1273	2.02×10^{7}	131.0	[9]
Co–Co	723–1023	7.20×10^{7}	117.2	[10]

Table 5
Arrhenius parameters for the volume diffusion of Co in Co quoted from the results in literature

	Temperature range (K)	$(D_v)_0$ ($\mu m^2\ h^{-1}$)	Q_v^{ef} (KJ $mole^{-1}$)	Reference
Co–Co(D_v)	772–1048	1.80×10^{10}	273.8	[11]
	1192–1297	6.10×10^{9}	260.4	[11]
	1047–1311	5.98×10^{10}	287.6	[12]

For comparison, the volume diffusion coefficients of Co in Co quoted from the data of Hirano et al. [11] were also listed in Table 3. Assumming the segregation factor S and grain boundary thickness δ in the three term value $S\delta D_b$ to be 1 and 10 Å respectively, it was shown that the real grain boundary diffusivities D_b were about eight orders of magnitude higher than the volume diffusivities of Co–Co in the temperature range from 833 to 1023 K. The Arrhenius plots of the grain boundary diffusion coefficients for both DP and DC reactions were shown in Fig. 8. Since the grain boundary diffusion data for Mo in Co was scarce in the literature, the results of W [8], Fe [9] and Co [10] in Co were taken for discussion. The related data were also ploted in Fig. 8. It was found that the curves for DP and DC reactions in the presented Co–6 at.% Mo alloy were quite consistent with those for grain boundary diffusions in Co–W and Co–Fe systems. They were about 1–2 orders of magnitude lower than the curve of Co–Co grain boundary self-diffusion. From the curves in Fig. 8 the pre-exponential factors $(S\delta D_b)_0$ and effective activation energies Q_b^{ef} were calculated and demonstrated in Table 4. It was shown that the effective activation energies for both DP and DC reactions were quite similar, which implied that the atom diffusion characteristics in this alloy during both reactions were similar. The data were higher than those obtained from the grain boundary diffusion of W, Fe and Co in Co. Compared with the volume diffusion parameters of Co–Co in Table 5 as quoted from the results of Hirano et al. [11] and Hassner and Lange [12], it was shown that the effective activation energies for the volume diffusion of Co in Co were obviously higher than the above cases of grain boundary diffusion. Summarizing these results, it can be concluded that the discontinuous precipitation and discontinuous coarsening reactions in Co–6 at.% Mo alloy were grain boundary diffusion-controlled.

4. Conclusions

Supersaturated solid Co–6 at.% Mo alloy isothermally aged at temperatures ranging from 773 to 1098 K were found to be decomposed by DP into a lamellar mixture of α' and β'' phases. At lower aging temperatures the precipitates grew with a regular lamellar structure, while at higher temperatures the β'' precipitates interacted with the stacking faults in the untransformed region in grain interiors to reveal a highly habit-oriented structure. The lamellar precipitates were subsequently decomposed into a coarser lamellar structure at all aging temperatures by a DC reaction. The growth rate of DC was about one or two orders of magnitude smaller than that of the DP reaction. The lamellar spacing ratios between DC and DP ranged from 5.8 to 6.2. Analysis of growth kinetics of DP and DC using the Petermann and Hornbogen theory suggested that the reactions were controlled by the grain boundary diffusion in the reaction fronts.

Acknowledgements

Partial financial support by National Science Council of ROC under contract number NSC 77-0405-EQ08-04 is greatly appreciated.

References

[1] W. Gust, Discontinuous Precipitation in Binary Metallic Systems, Proc. Phase Transformations, Printed by the Chamelton Press, London, 1979, pp. 1127–1176.
[2] R.A. Fournelle, Acta Metall. 27 (1979) 1135–1145.
[3] W. Gust, B. Predel, S.N. Mehra, Mater. Sci. Eng. 21 (1975) 131–138.
[4] R. Lück, Z. Metallk. 66 (1975) 488–491.

[5] W. Gust, T.H. Chuang, B. Predel, in: P. Haasen, V. Gerold, R. Wagner, M.F. Ashby (Eds.), Decomposition of Alloys: The Early Stages, Proceedings of the Second Acta-Scripta Metallurgica Conference, Pergamon Press, 1983, pp. 208–213.
[6] J. Petermann, E. Hornbogen, Z. Metallkd. 59 (1968) 814–822.
[7] A.M. Beltran, Cobalt-base alloys, in: C.T. Sims, N.S. Stoloff, W.C. Hagel (Eds.), Superalloys II, John Wiley and Sons, 1987, pp. 142–143.
[8] L.N. Larikov, L.F. Chernaya, O.A. Shmatko, Metallofiz. 28 (1969) 85–98.
[9] M. Aucounturier, P. Lacombe, Kobalt 28 (1965) 111–118.
[10] V.B. Brik, L.N. Larikov, V.M. Falchenko, Ukrain. Fiz. Zhur. 20 (1975) 397–404.
[11] K. Hirano, R.P. Agarwala, B.L. Averbach, M. Cohen, J. Appl. Phys. 33 (1962) 3049–3054.
[12] A. Hassner, W. Lange, Phys. Stat. Solidi. 8 (1965) 77–91.
[13] C.F. Yang, G. Sarkar, R.A. Fournelle, Acta Metall. 36 (1988) 1511–1520.
[14] I. Manna, J.N. Jha, S.K. Pabi, J. Mater. Sci. 31 (1996) 2401–2407.
[15] T.H. Chuang, W. Gust, B. Predel, R.A. Fournelle, Mater. Sci. Eng. A112 (1989) 175–183.
[16] T.H. Chuang, R.A. Fournelle, W. Gust, B. Predel, Acta Metall. 36 (1988) 775–785.
[17] S.P. Gupta, S. Singh, Z. Metallkd. 87 (1996) 740–747.
[18] S. Mitao, L.A. Bendersky, Acta Metall. 45 (1997) 4475–4489.
[19] G.W. Qin, S.M. Hao, Scripta Mater. 37 (1997) 937–942.
[20] Y. Suzuki, T. Suzuki, T. Tsujimoto, J. Jpn. Inst. Metals 61 (1997) 678–683.
[21] Y. Suzuki, T. Suzuki, T. Tsujimoto, J. Jpn. Inst. Metals 61 (1997) 684–689.
[22] L.E. Murr, in: Interfacial Phenomena in Metals and Alloys, Addison-Wesley, London, 1975, p. 131.
[23] W.B. Pearson, in: A Handbook of Lattice Spacings and Structures of Metals and Alloys, Pergamon Press, London, 1958.